General Disclaimer

One or more of the Following Statements may affect this Document

- This document has been reproduced from the best copy furnished by the organizational source. It is being released in the interest of making available as much information as possible.

- This document may contain data, which exceeds the sheet parameters. It was furnished in this condition by the organizational source and is the best copy available.

- This document may contain tone-on-tone or color graphs, charts and/or pictures, which have been reproduced in black and white.

- This document is paginated as submitted by the original source.

- Portions of this document are not fully legible due to the historical nature of some of the material. However, it is the best reproduction available from the original submission.

Produced by the NASA Center for Aerospace Information (CASI)

NASA Technical Memorandum 83362

Processing of Fused Silicide Coatings for Carbon-Based Materials

(NASA-TM-83362) PROCESSING OF FUSED SILICIDE COATINGS FOR CARBON-BASED MATERIALS (NASA) 39 p HC A03/MF A01 CSCL 11C

N83-27019

Unclas
G3/27 03960

James L. Smialek
Lewis Research Center
Cleveland, Ohio

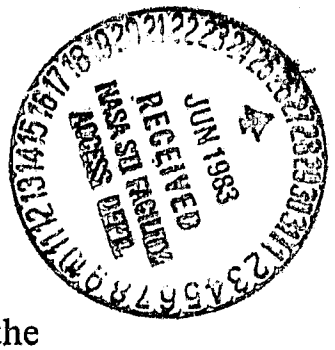

Prepared for the
Ceramic-Metal Systems Division Conference of the
American Ceramic Society Meeting
Cocoa Beach, Florida, January 19–24, 1983

NASA

PROCESSING OF FUSED SILICIDE COATINGS FOR CARBON-BASED MATERIALS

James L. Smialek

National Aeronautics and Space Administration
Lewis Research Center
Cleveland, Ohio 44135

E-1624

ABSTRACT

The processing and oxidation resistance of fused Al-Si and Ni-Si slurry coatings on ATJ graphite was studied. Al-Si coatings could not be successfully produced nor were they protective. Ni-Si coatings in the 70 to 90 percent Si range were successfully processed to melt, wet, and bond to the graphite. The molten coatings also infiltrated the porosity in graphite and reacted with it to form SiC in the coating. Cyclic oxidation at 1200° C showed that these coatings were not totally protective because of local attack of the substrate, due to the extreme thinness of the coatings in combination with coating cracks.

INTRODUCTION

Coated carbon composite materials are currently used as the heat shield for the space shuttle nose cap and wing leading edges.[1] These carbon-carbon composites are also being considered for various high temperature parts of aircraft turbine engines, such as exhaust nozzles. The major advantage of such materials is the very high strength-to-weight ratios at temperatures between 1200° to 2000° C.[2] One major disadvantage of carbon-based materials is the extremely high oxidation rate. For this reason these materials are coated with SiC, generally applied by chemical vapor deposition or pack cementation

processes. These coatings are quite protective above 1200° C where a fluid SiO_2 glass is formed as the protective oxide. At lower temperatures, cracks in the coating, caused by differential thermal expansion, cannot be sealed by the SiO_2 glass because it is too viscous.[3,4,5] Thus, catastrophic lower temperature oxidation of the substrate is common.

The purpose of the present study was to investigate the possibility of producing oxidation resistant silicon-based coatings on graphite by a fused slurry technique. This process has the potential to penetrate any porosity in the substrate and to act as an oxidation-resistant additive in addition to providing an oxidation resistant outer layer. These coatings are very low cost, have compositional flexibility, and could be easily applied as repair coatings to local damaged areas. This study concentrated on mapping the compositions and sintering temperatures that produce dense, fused coatings that wet, bond, and react with the substrate. The coatings were characterized by SEM, XRD, and optical metallography, and they were then oxidation tested at 1200° C.

EXPERIMENTAL PROCEDURE

Coupons of ATJ graphite were machined to a size of 0.25 x 1.25 x 2.50 cm. The graphite was 73 percent dense and exhibited a substantial amount of large porosity, Fig. 1. Slurry mixtures of Al + Si or Ni + Si powders (-325 mesh) were made using a nitrocellulose lacquer vehicle. The slurries were sprayed onto the coupons, allowed to air dry, and vacuum sintered between 1100° and

1500° C at 10^{-5} torr (10^{-6} MPa). The coupons were sintered while resting on an Al_2O_3 plate or suspended from an Al_2O_3 hanger rod. Some specimens were cyclicly oxidized in a vertical tube furnace at 1200° C in 1 atm. air using 1 hr heating cycles. Both as-sintered and as-oxidized specimens were examined by XRD, SEM, and optical microscopy for coating phases and microstructure.

RESULTS AND DISCUSSION

Insofar as this study is an optimization program, the results are presented in a sequential manner giving the conclusions and recommendations of each experiment separately. Basically four processing experiments were conducted: a preliminary study of only two Al-Si and Ni-Si compositions each, a study of compositional variations over much of the Ni-Si binary system, an optimization study of the sintering procedure for the Ni-70 Si (weight percent) coating, and an additional compositional optimization in the 70 to 90 percent Si range.

A. Trial Al-Si and Ni-Si Coatings

As a preliminary experiment, low-melting compositions of Al-Si and Ni-Si slurry coatings were sintered while lying on an Al_2O_3 plate at 1300° C for 2 hours. The eutectic compositions, Al-12 Si (T_{mp} = 577° C) and Ni-29 Si (T_{mp} = 964° C), were chosen in an attempt to maximize the fluidity of the fused coating and to ensure infiltration of porosity. Al-50 Si and Ni-50 Si

coatings were also tried to determine the effects of higher Si contents. A summary of these processed coatings is shown in table I. The Al-Si compositions lost considerable coating weight due to volatilization during vacuum sintering. X-ray diffractometer scans of the coating surface showed that only the Al-50 Si coating showed appreciable reaction with the graphite to form SiC. Both coatings exhibited a rather porous external surface indicating that melting, flow, and wetting did not occur.

The Ni-Si coatings did not lose nearly as much weight. They also exhibited melting and wet the substrate, but were so fluid that the coating ran excessively to the backside of the specimen. Only the Ni-50 Si coating contained SiC as a major coating constituent.

The microstructures of these coatings are shown in Fig. 2. The Al-12 Si coating has very little metallic coating phase or reaction zone apparent. The Al-50 Si coating has more metallic coating phase present in an external layer as well as in the pores of the substrate. This is also true of the Ni-Si coatings. These coatings show penetrations of 300 μm; however, the external coating is only 10 μm thick and is not exceptionally uniform.

The cyclic oxidation behavior at 1200° C is shown in Fig. 3. Very little protection of the graphite substrate was offered by any of the coatings. Visual inspection showed the Al-Si coatings to be uniformly attacked by the oxidation exposure as would be expected for a thin porous structure. The Ni-Si coatings themselves, however, appeared to be quite oxidation resistant: they were metallic in appearance with only a thin tarnish oxide layer. The failure mode of the Ni-Si coated graphite was by local attack of the specimen backside, where wetting and coverage was poor, and where the slurry had formed discrete molten globules rather than a uniform layer.

The same four coatings were also processed using a 1200° C, 2 hr sintering schedule in order to reduce the vaporization losses of the Al-Si coatings and the excess fluidity of the Ni-Si coatings. However, no appreciable change in the coating appearance, coverage, or oxidation resistance was observed. It therefore appeared that the Al-Si coatings were not processed as easily as the Ni-Si coatings and that it might be possible to prepare less-fluid Ni-Si coatings by using higher melting point slurry mixtures.

B. Compositional Variations in the Ni-Si System

The partial success of the Ni-Si coatings warranted further investigation into more Ni-Si coating compositions. An attempt to limit excessive flow and coating loss due to pore penetration was made by shortening the sintering time to 5 min., decreasing the coating deposits to 25 mg/cm^2, and by indexing the sintering temperature to the liquidus temperature of the coating composition (e.g. $T_s = T_{m.p.} + 20°$ C). The parameters of this coating study are shown in table II.

Ni-29 Si and Ni-50 Si coatings sintered at 985° and 1145° C, respectively, did not wet and were prone to cracking and delamination (not shown in table II). Duplicate samples processed at 1200° C were subject to excessive flow despite the short time and reduced coating thickness.

In contrast, the Ni-70 Si coating showed excellent wetting, flow, and coverage. It appeared as a uniform bright, reflective, metallic outer layer with only slight indication of excess build-up on the specimen underside. XRD also indicated that a substantial amount of SiC had been formed at 1325° C which, along with metallic Si, would be useful for its oxidation resistance.

The high Si compositions did not exhibit a metallic fused external coating surface and therefore showed no problems with excess flow. However, they did appear to be somewhat porous visually. All these coatings formed substantial amounts of SiC, with some Si and Ni-Si phases.

As-sintered Si-rich coatings are shown in Fig. 4. The Ni-70 Si coating shows a substantial amount of smooth fused coating surface, which, from XRD analysis, is most likely metallic Ni-Si compounds and Si. The small particles with crystallographic facets are then likely to be SiC which formed from reaction with carbon which had diffused outward from the substrate. Some coating cracks were observed at lower magnifications. The Ni-90 Si coating shows a substantial increase in the number of crystals which appear to be well-sintered together, possibly by a prior liquid phase. The 100 percent Si coating appears only partially sintered and deep depressions between the crystallite agglomerates are apparent. These depressions and the lack of complete sintering may provide enough gas paths for direct oxidation of the substrate. The reason why Ni-90, 95, and 100 Si coatings appeared sintered and not fused, even when processed above the melting point of the coating, is not known. Probably most of the molten coating had infiltrated pores, leaving only the Si which reacted to form SiC.

The microstructure of the Ni-70 Si coating in cross-section is shown in Fig. 5. This is an intact area of the coating after oxidation at 1200° C for 5 hrs, but serves to illustrate the as-sintered coating structure and phases as well. An outer 10μm layer of reasonably continuous and uniform SiC, Ni-Si, and Si coating is apparent. The pores near the surface have been filled with a liquid Ni-Si phase to a depth of about 180 μm. The external layer and the filled pores of both these areas show some internal structures which are probably SiC precipitates. A microprobe study of these areas showed high levels of Ni in the penetrated pores with amounts of Si consistent with the formula

for Ni_2Si. In this phase the carbon content was very low. In adjacent phases the Si and C contents were more consistent with SiC, and the Ni content was low. The dark areas between the filled pores showed only C with a trace of Si and no Ni.

Microstructural examination (Fig. 6) showed that the Ni-29 Si and Ni-50 Si coatings were non-uniform and that substantial oxidation of the underlying graphite occurred. The Ni-70 Si coating by comparison is quite intact as discussed previously. The Ni-90 Si, Ni-95 Si, and 100 Si coatings all show a substantial amount of pore penetration by a liquid phase as well as some coverage by a fused surface layer which was not evident from the SEM observations. The penetration depth increased with the sintering temperature of each of these specimens. However, the external layers were apparently not fully sintered as substantial oxidation of the graphite is evidenced by the excessive subsurface porosity.

The outer surfaces of the oxidized specimens were also examined by SEM. As shown in Fig. 7, the Ni-70 Si coating was generally quite uniform with a textured surface of small oxide needles. In the particular area shown, the coating had cracked off and revealed the Ni-Si globular penetrations. The Ni-90 Si coating still showed discreet SiC crystallites, whereas the Ni-95 Si coating appeared to be covered by a layer of glassy oxide. The oxide phases could not be conclusively identified because post-test XRD only showed a weak pattern for SiO_2 α-crystobalite. No glassy SiO_2 peak was observed in the XRD pattern. Some Al_2O_3 was also found for Ni-70 Si and Ni-95 Si which was probably due to contamination from the Al_2O_3 tubes in the oxidation furnace.

The weight change data for the oxidation test is shown in Fig. 8. Both the Ni-29 Si and Ni-50 Si specimens were so badly attacked that testing was stopped after one hour. The Ni-50 Si coating itself appeared quite oxidation resistant, but the delamination and lack of coverage on the specimen underside caused its poor performance. The Ni-70 Si and Ni-90 Si coatings both had the most intact outer coating layer; thus these exhibited the most protection. The failure of these coatings may have been due to fine coating cracks. Failure started at coating edges and corners for both the Ni-70 Si coatings. The 100 Si coating was apparently porous as the coating failed in a uniform manner.

A relationship between the coating behavior and coating composition could be surmised from the gravimetric curves. This dependence is shown more clearly in Fig. 9, where the rate of weight change is plotted against coating composition. The best performance is indicated to be between 70 and 90 percent Si, as would be expected for the coatings showing the best coverage with a dense external layer. The higher Si coatings showed less protection due to the porous sintered nature of the external layer. Coating compositions in the Ni-70 Si to Ni-90 Si range, however, were extremely thin and sensitive to either the fine cracks or imperfect coverage at the edges. Also, flow of the coating to the specimen underside is very detrimental because this results in a thinner overall coating.

C. Optimization of the Ni-70 Si Coating Sintering Schedule

Thicker external coatings are needed which are not compromised by excessive flow to the underside of the specimen. The first attempt to remedy this problem was to lower the sintering temperature below the liquidus temperature (1305° C) as indicated in table III, part (a). Also the original 50 mg/cm^2

coating thickness was used, and the specimens were hung from an Al_2O_3 rod through a hole in the specimen rather than rested on an Al_2O_3 plate. Excessive flow also occurred for these specimens, even though some had not fully fused, as evidenced by molten areas with residual solid (slush).

Consequently the sintering temperature was lowered even further, but the time was increased to one hr to allow the fusion, wetting, and infiltration process to occur completely and dissolve any residual solids, (table III, part (b)) The first three specimens showed that 1100° and 1150° C were too low for this to occur, but one hr at 1200° C produced an excellent coating in terms of wetting, uniformity, and fluidity. The changeover from partial to total fusion between 1100° and 1200° C can be seen in Fig. 10(a). What appeared visually as a very rough-textured, partially-sintered coating at 1100° C is seen to have some liquid phase sintering and particle agglomeration. At 1150° C discreet areas have fused and "wicked-in" to the substrate pores leaving depressed flat areas. At 1200° C the entire coating has melted to a uniform surface. At higher magnifications (Fig. 10 (b)), the surface of the 1100° and 1150° C coating agglomerates can be seen to be quite smooth on a miroscale, whereas the 1200° C coating is textured due to the small faceted SiC crystallites.

The trend in the phase constituency with low sintering temperatures is shown in Fig. 11. Here relative amounts of phases were estimated by summing the intensity of all peaks up to $2\theta = 80°$ and ratioing the summed intensity for one phase to that of the total sum. From this it is clear that substantial amounts of Si and Ni-Si compounds exist after one hr at 1200° C. Thus a double sintering step was employed to cause more complete reaction to form SiC. The 1200° C pre-sinters allowed optimum melting and wetting, and subsequent reacting at 1325° C allowed more SiC to form without excessive flow. An increased density of SiC crystallites was observed microscopically,

and the consumption of Si to form SiC is also indicated in Fig. 11.

The effect of the second sintering step on coating quality is indicated in table III, part (b). The reflective metallic coating resulting from the 1200° C pre-sinter was transformed to a non-metallic surface when sintered at 1250° to 1375° C. No apparent flow of the original coating took place. The resultant coating was very uniform and appeared preferable to the single-step 1325° C sintered coating exhibiting excessive flow. At 1450° C the coating exhibited remelting to again form a reflective metallic surface and there was a slight buildup of coating at the bottom of the specimen.

The estimated phase constituency of the two step coatings is shown in Fig. 12. The 1200° C/1 hr + 1200° C/1 hr sample contained a relatively large amount of the Ni-Si compounds compared to single-step coatings (Fig. 11). The 1200° C/1 hr + 1325° C/1 hr sample indicted a major decrease in the amount of the metallic phase, and a corresponding increase in the SiC phase. The 1200° C/1 hr + 1450° C/1 hr sample indicated again a large amount of Ni-Si compounds which is consistent with the observed remelting and lack of SiC crystallites at the surface. The surfaces of the Ni-70 Si coating sintered by the two-step process is shown in Fig. 13. In general, all the sintering temperatures produced coatings with a fused outer coating of Ni-Si compounds decorated with small crystals of SiC. The 1325° C sample, however, appeared roughest at low magnifications and had the highest concentration of SiC crystals at the surface. Also this coating did not exhibit any cracks, as opposed to the two others which had numerous cracks, spaced 100 μm apart.

The oxidation resistance of the two-step coatings is shown in Fig. 14. The 1325° C coating showing no re-melting, flow, or cracks, and having the highest SiC content provided the best oxidation protection. This sample was

grey and appeared quite uniform after oxidation. The 1200° and 1450°C samples had nearly the same oxidation resistance, as might be expected from their similar appearance, microstructure, and phases. The 1200° C coating appeared metallic or light grey-blue and quite oxidation resistant except for a pinhole through the coating formed at 4 hr. The same was true for the 1450° C sample except for a pinhole formed at 2 hr. Yellow tinted oxide was also apparent after 10 hr. The 1250° C sample which had the poorest oxidation resistance, appeared tan with dispersed yellow and blue areas.

The rate of weight change as a function of the final sintering temperature is shown in Fig. 15. These rates were determined from the slope of the gravimetric curves averaged over the majority of the test. In general a broad maximum appears near the 1325° C area, however the 1250° C sample deviates from this trend. The reason for this is not known.

Failure appears to be controlled by local defects which may be caused by the extreme thinness of the external coating as well as by the network of fine coating cracks in the case of the 1200° and 1450° C samples. The oxide phases formed after oxidation were determined by XRD. All four coatings formed primarily NiO; only a weak pattern for crystalline SiO_2 could be resolved.

The microstructure of the oxidized Ni-70 coatings is shown in Fig. 16. The cracks formed after sintering are still apparent in the 1200° and 1450° C specimens. These cracks have not healed by SiO_2 glassy formation and could therefore be a major contribution to coating failure. All the coatings exhibited faceted NiO crystals which were 1 to 2 μm for the 1200° C coating and up to 10 μm for the 1325° and 1450° C coating. NiO is known to grow rapidly at 1200° C, and this oxide formation would eventually lead to wearout of the thin coatings without protective SiO_2 formation.[6] Again the 1325° C specimen

exhibited no obvious cracks or holes and the failure mechanism of this coating is not clear.

D. Compositional Modifications in the Ni-70 Si to Ni-90 Si Range

Slight modifications to the Ni-70 Si composition were also studied concurrently with the prior experiment. It was desired to determine whether increased Si contents could decrease the coating flow while still allowing melting and wetting to occur. Another motivation was to study the performance of various compositions processed by the two-step method. The single-step coatings, table IV, part (a), were sintered at 1400° C for only 5 minutes to minimize liquid running. The 70 and 75 percent Si coatings both fused to a metallic luster and ran to the bottom of the specimens, while the 85 percent Si coating appeared uniform, but not densely fused. X-ray diffraction data from these specimens showed that the fused 75 percent and 85 percent Si coatings were primarily Si, while the Ni-85 Si coating was primarily SiC, Fig. 17. The Ni-85 Si data shown here was obtained after heating to 1450° C for 5 min. and from a duplicate sample reheated to 1450° C for 6 hr. Neither coating showed any external signs of fusion, with either this higher temperature or longer-time sinter, but appeared uniformly grey, textured, and non-metallic. The only effect of the extra sintering time was to slightly increase the amount of SiC.

The coatings processed by the two-step procedure (table IV, part (b)) were all uniform non-metallic grey, and showed no signs of excessive coating flow. Thus the two-step process again allowed for good coverage, but the density of the sintered coating may be in question. The trend in coating phase variation with composition is shown in Fig. 18. Wide scatter bands for

multiple specimens were observed, but in general the SiC phase increased with percent Si while the Ni-Si phases decreased.

The surfaces of the high-silicon coatings sintered by the two-step process is shown in Fig. 19. All the coatings exhibit a rather porous open sintered structure with some faceted particles plus fine spherical particles. No cracks were observed. At low magnifications some very deep voids in the coating can be found for all three compositions. These are probably near areas of high porosity in the substrate where much of the molten coating has penetrated the graphite, leaving behind a hole in the coating. This type of defect was not noticed in the Ni-70 Si coatings where complete wetting and flow occurred for all temperatures $\geq$ 1200° C.

The oxidation behavior, Fig. 20, shows the high Si content coatings to be the most protective. The uniform appearance of these specimens indicated that they did not degrade in the localized defect mode as did the Ni-70 coatings of Fig. 14. The 75 percent Si coating was generally yellow-grey throughout the oxidation test; the 80 percent Si began as blue-grey and became slightly tan at 10 hr; the 85 percent Si began as a very dark charcoal grey, changing to a slightly blue-green tint at 10 hr.

The rate of weight change as a function of coating composition is shown in Fig. 21. In general the 70, 80, and 85 percent Si coatings all exhibited nearly equivalent protection. The reason for the minimum at 75 percent Si is not known, although the major difference in microstructure from fused to sintered occurs at 70 to 75 percent Si. Except for Ni-75 Si, these rates of weight changes are similar to those observed in a 5 hr oxidation test of the single-step coating (Fig. 9).

The oxide phases formed on the Ni-75 Si and Ni-80 Si coatings were identified by XRD to be primarily NiO with some SiO_2 possible. The Ni-85 Si

coating had only a weak SiO_2 pattern with no NiO which may account for the improved oxidation resistance. The surface structure of the oxidized coatings is shown in Fig. 22. The faceted NiO crystallites are apparent in the Ni-75 Si and Ni-80 Si coatings, but not in the Ni-85 coating. The Ni-85 coating also appears to be covered with a molten material, such as glassy SiO_2, which was not apparent in the as-coated condition (Fig. 19). The sealing effect of such a glass plus the lack of NiO may be related to the better protection of this coating. It should also be noted that none of the high-silicon coatings showed obvious cracks before or after oxidation.

SUMMARY AND CONCLUDING REMARKS

Al-Si and Ni-Si powder mixtures were applied to ATJ graphite substrates as slurry coatings and vacuum sintered. The coatings were evaluated by metallography, SEM, XRD, and 1200° C cyclic oxidation. Initial experiments showed that the Al-Si coatings evaporated extensively during sintering and provided incomplete coverage. The poor 1200° C oxidation resistance of these coatings indicated that Al-Si compositions were not easily processed as coatings for graphite.

Ni-Si coatings did not evaporate extensively and could be processed to provide a uniform outer layer of Si, SiC, and Ni-Si compounds. While all Ni-Si compositions were found to melt and infiltrate the large amount of porosity in the graphite, only some of the compositions and sintering schedules resulted in a dense external coating which could provide any amount of protection. These compositions lie in the region of about Ni-70 Si to Ni-90 Si. Sintering Ni-70 Si at 1200° C resulted in a uniform fused coating which

exhibited excellent wetting and minimal fluid flow. Lower temperatures resulted in an incompletely melted coating, while higher temperatures resulted in excessive flow and build-up of the coating at the bottom of the specimen. SEM and XRD analyses of these coatings showed that the amount of SiC increased from zero at 1100° C to ~50 percent at 1325° C in the form of faceted 5 μm crystallites. While the oxidation resistance of the coatings themselves appeared excellent, the protection was inadequate due to localized failures. It is expected that coating cracks or an area with an especially thin outer layer may have been the cause of these failures.

A two-step sintering process successfully produced uniform coatings which were fused to allow wetting and infiltration to occur at 1200° C and then heated to 1325° C to convert more of the coating to SiC. While these coatings appeared to be processed optimally, the oxidation resistance was inadequate due to some unidentified local failures. Two-step processing at 1200°/1450° C resulted in remelted coatings which cracked and were not protective and also formed much NiO. The ultimate success of the Ni-70 Si coating on porous ATJ graphite may thus be in question, regardless of what sintering schedule is used.

More protection was shown by the high silicon coating, Ni-85 Si, which did not exhibit a dense fused outer metallic layer, but was more granular and porous. The advantage of this coating may be that it was not cracked, nor did it form NiO. Further sintering studies of the Ni-85 Si coating, especially utilizing higher temperatures to cause more complete sintering, appear to be warranted.

While this study elucidated the behavior of various Ni-Si slurry coatings processed by a number of sintering schedules, it did not lead to a workable oxidation-resistant coating. It is believed that the single most important

reason for the inadequate oxidation protection is the high degree of interconnected porosity in the substrate. This causes most of the coating to infiltrate pores, leaving less than 25 μm as an outer layer. Thus for ATJ graphite, thicker slurry coatings should be very beneficial (if they can be more successfully sprayed without craze cracking and sintered without excessive rundown). However, high density carbon-carbon composites may be successfully coated without the need for thick coatings.

REFERENCES

1. P. R. Becker, "Leading-Edge Structural Material System of the Space Shuttle," Am. Ceram. Soc. Bull., 60, 1210-1214 (1981).
2. E. Fitzer, M. Heym, "High-Temperature Mechanical Properties of Graphite and Carbon," High Temp. High Pressures, 10, 29-66 (1978).
3. D. M. Curry, H. C. Scott, C. N. Webster, pp. 1524-1539 in The Enigma of the Eighties: Environment, Economics, Energy, Vol. 24, Book 2, SAMPE, Azusa, Ca., (1979).
4. S. C. Singhal, Oxidation Kinetics of Hot-Pressed Silicon Carbide," J. Mater. Sci., 11, 1246-1253 (1976).
5. F. F. Lange, "Healing of Surface Cracks in SiC by Oxidation," J. Am. Ceram. Soc., 53 (5) 290 (1970).
6. C. E. Lowell, S. J. Grisaffe, D. L. Deadmore, "Oxidation of TD Nickel at 1050 and 1200° C as Compared to Three Grades of Nickel of Different Purity," Oxid. Met., 4, 91-111 (1972).

ORIGINAL PAGE IS
OF POOR QUALITY

TABLE I. - TRIAL Al-Si AND Ni-Si COATINGS

[1300° C, 2 hr.]

Composition, weight percent	Coating weight, mg/cm^2		Phases	Appearance
	Green	Sintered		
Al-12 Si	25	4	C, Al_2C_3, SiC	Sintered, porous
Al-50 Si	50	9	SiC, C	Sintered, porous
Ni-29 Si	50	46	U, C, (SiC)	Fused, metallic, coating ran
Ni-50 Si	50	45	SiC, C	Fused, metallic, coating ran

U = Unidentified Ni-Si compounds.

( ) = Low intensity peaks.

TABLE II. - COMPOSITIONAL STUDIES OF Ni-Si COATINGS

[25 mg/cm^2, sintered for 5 min.]

Composition, weight percent	Sintered coating weight, mg/cm^2	Temperature, °C		Phases	Appearance
		T_{mp}	T_s		
Ni-29 Si	23	964	1200	Ni_2Si, C, U	Fused, coating ran
Ni-50 Si	24	1125	1200	C, Si, U	Fused, metallic, delaminated
Ni-70 Si*	23	1305	1325	SiC, Si, U, C	Fused, metallic, excellent wetting, coating ran
Ni-90 Si	22	1395	1415	SiC, C, Si, U	Sintered, grey matte
Ni-95 Si	22	1410	1450	SiC, C, U	Sintered, grey matte
100 Si	20	1417	1437	SiC, C, Si	Sintered, grey matte

U = Unidentified Ni-Si compounds.

ORIGINAL PAGE IS
OF POOR QUALITY

TABLE III. - OPTIMIZATION OF Ni-70 Si SINTERING SCHEDULE

(a) Single-step process

[50 mg/cm^2.]

T, t Sinter	Phases	Appearance
1255° C, 5 min	Si, U, SiC	Partial fusion, metallic, excessive flow
1280° C, 5 min	Si, SiC, U	Partial fusion, metallic, excessive flow
1325° C, 5 min	Si, SiC, U, C	Fused, metallic, excessive flow
1400°C, 5 min	Si, SiC, U	Fused, excessive flow

(b) Two-step process optimization

T, t, Sinter	Phases	Appearance
1100° C, 1 hr	Si, (SiC, U)	Partial sintering, rough matte, minimal fusion
1150° C, 1 hr	Si, SiC, (U)	Sintered, partial fusion, metallic
1200° C, 1 hr	SiC, Si, U	Fused, metallic, optimum wetting, no flow
1200° C/1 hr + 1200° C/1 hr	U, SiC, Si	Fused, metallic, optimum wetting, no flow
1200° C/1 hr + 1250° C/1 hr	U, SiC, (Si)	Fused and reacted to grey matte, no flow
1200° C/1 hr + 1325° C/1 hr	U, SiC	Fused and reacted to grey matte, no flow
1200° C/1 hr + 1375° C/1 hr	U, SiC	Fused, metallic matte, no flow
1200° C/1 hr + 1450° C/1 hr	U, SiC	Fused, metallic, remelting and some flow

U = Unidentified Ni-Si compounds.

( ) = Low intensity peaks.

ORIGINAL PAGE IS
OF POOR QUALITY

TABLE IV. - SECOND COMPOSITIONAL OPTIMIZATION IN THE Ni-70 Si RANGE

(a) 1400° C, 5 min single step process

Composition	Phases	Appearance
Ni-75 Si	Si, SiC	Metallic, fused, excessive flow
Ni-80 Si	Si, SiC	Metallic, fused, excessive flow
Ni-85 Si	SiC, Si	Sintered, grey, no flow

(b) -1200° /1 hr + 1325° C/1 hr two-step process

Ni-75	SiC, U	Nonmetallic, dark grey, partial sintering; no flow
Ni-80 Si	SiC, U	Nonmetallic, dark grey, partial sintering; no flow
Ni-85 Si	SiC, U	Nonmetallic, dull grey, minimal sintering no flow

ORIGINAL PAGE IS
OF POOR QUALITY

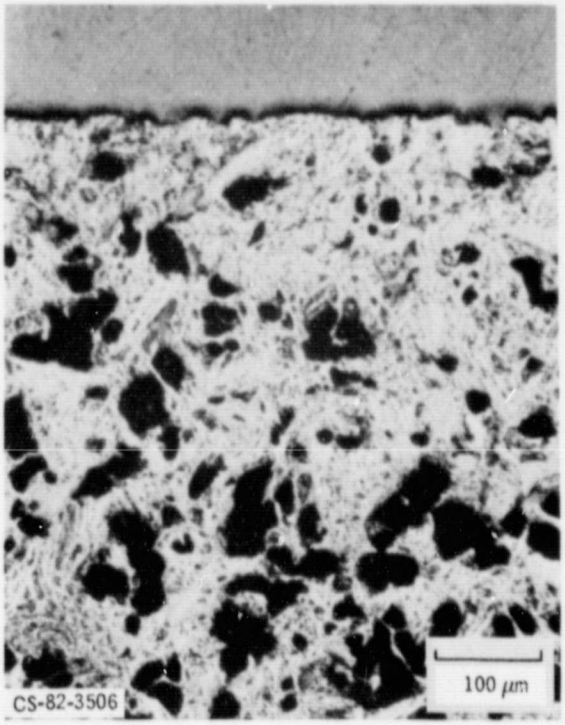

Figure 1. - Porous microstructure of as-received ATJ graphite.

ORIGINAL PAGE IS
OF POOR QUALITY

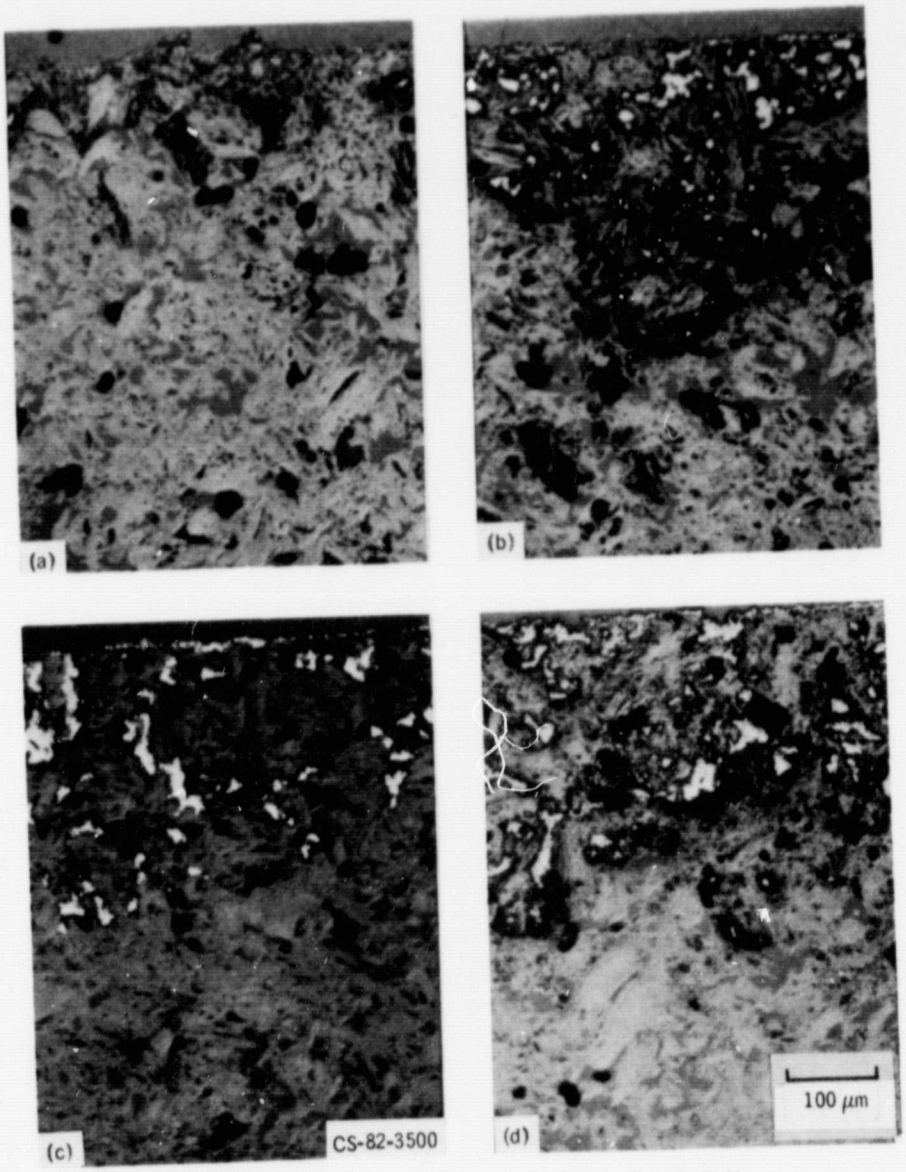

(a) Al-12 Si.
(b) Al-50 Si.
(c) Ni-29 Si.
(d) Ni-50 Si.

Figure 2. - Microstructures of Al-Si and Ni-Si coatings on ATJ graphite sintered at 1300 C, for 2 hour.

ORIGINAL PAGE IS
OF POOR QUALITY

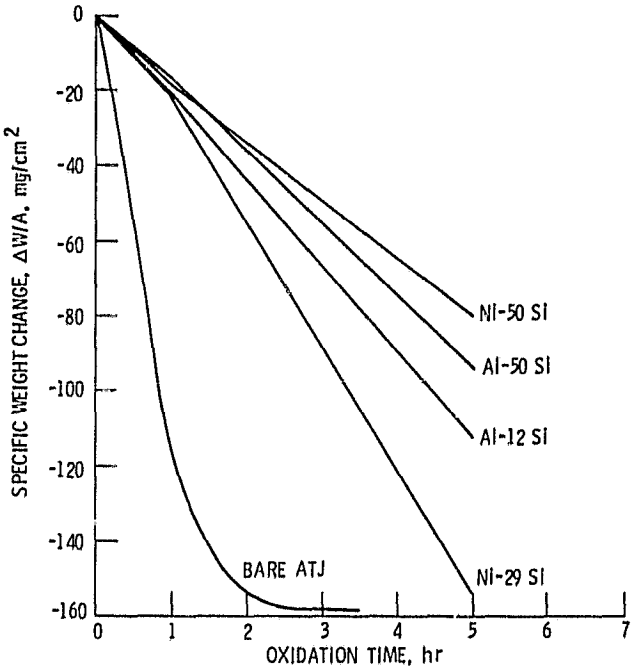

Figure 3. - 1200° C cyclic oxidation of Al-Si and Ni-Si coatings.

ORIGINAL PAGE IS
OF POOR QUALITY

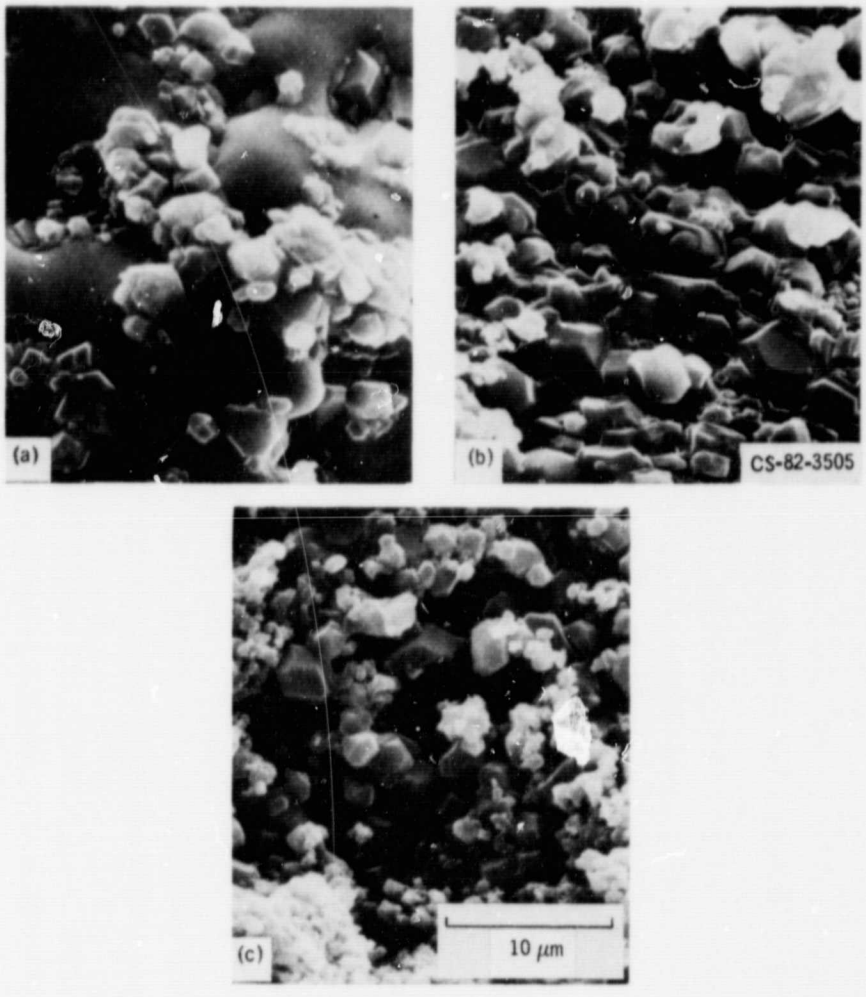

(a) Ni-70 Si, T_s = 1325 C.

(b) Ni-90 Si, T_s = 1430°C.

(c) 100 Si, T_s = 1437 C.

Figure 4. - Effect of coating composition surface structure for as-sintered Ni-Si coatings.

ORIGINAL PAGE IS
OF POOR QUALITY

Figure 5. - Cross-section of Ni-70 Si coating processed at 1325° C/5 min. and oxidized at 1200° C for 5 hr. Coating has penetrated pores and the outer layer has protected the unreacted graphite in most areas.

ORIGINAL PAGE IS
OF POOR QUALITY

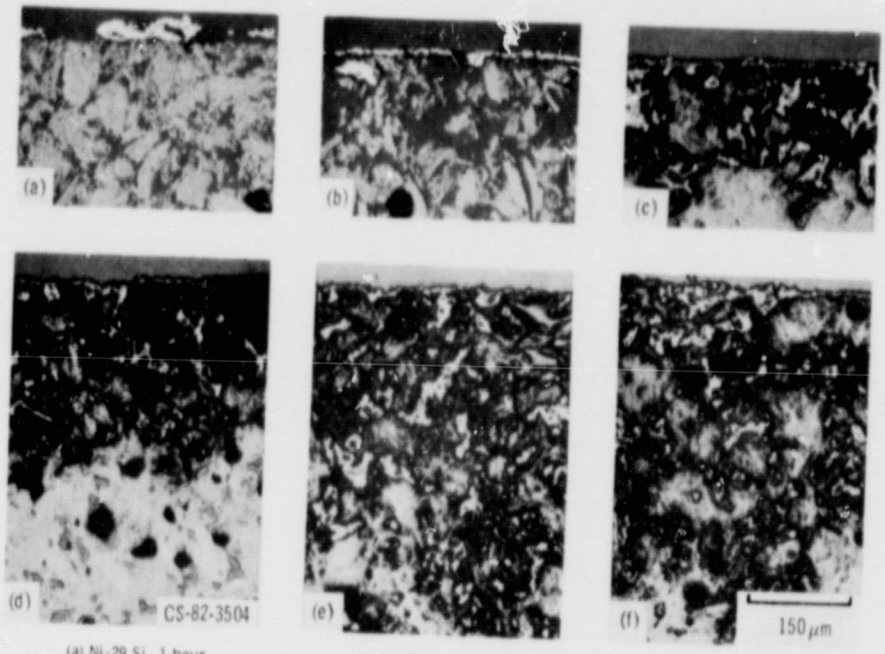

(a) Ni-29 Si, 1 hour.
(b) Ni-50 Si, 1 hour.
(c) Ni-70 Si, 5 hour.
(d) Ni-90 Si, 5 hour.
(e) Ni-95 Si, 5 hour.
(f) 100 Si, 5 hour.

Figure 6. - Effect of coating composition on microstructure and protection in 1200 C oxidation.

ORIGINAL PAGE IS
OF POOR QUALITY

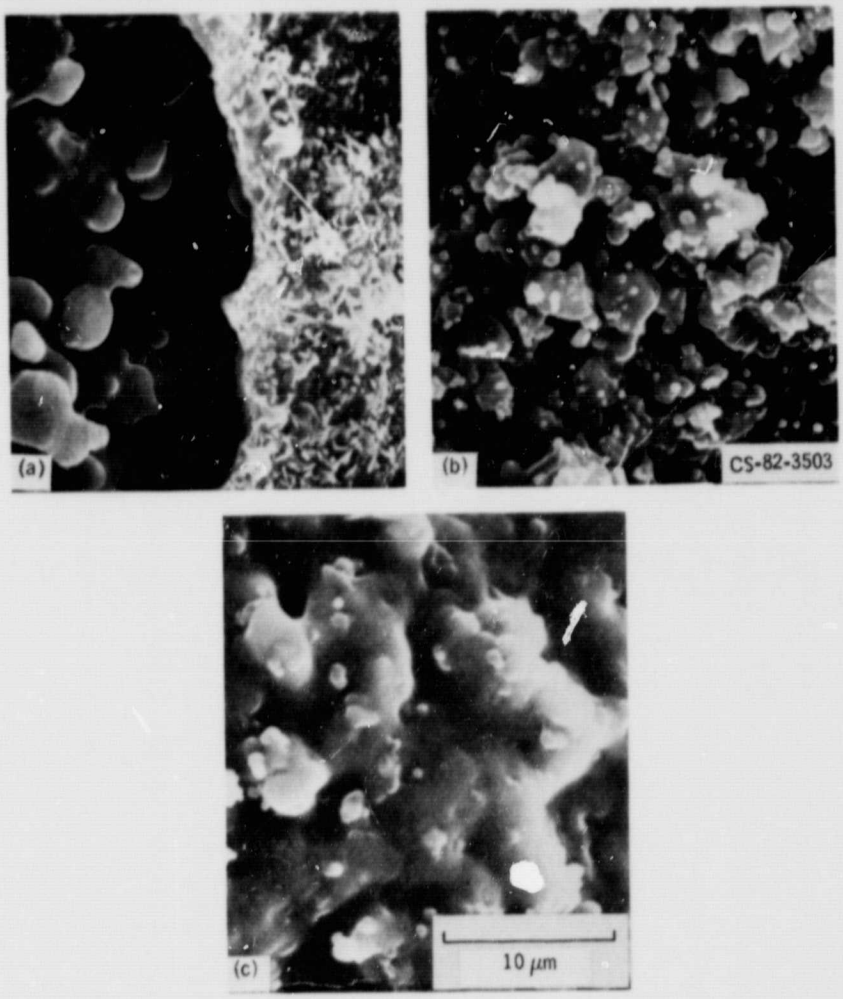

(a) Ni-70 Si.

(b) Ni-90 Si.

(c) Ni-95 Si.

Figure 7. - Surface structure of Ni-Si coatings oxidized at 1200°C for 5 hours.

ORIGINAL PAGE IS
OF POOR QUALITY

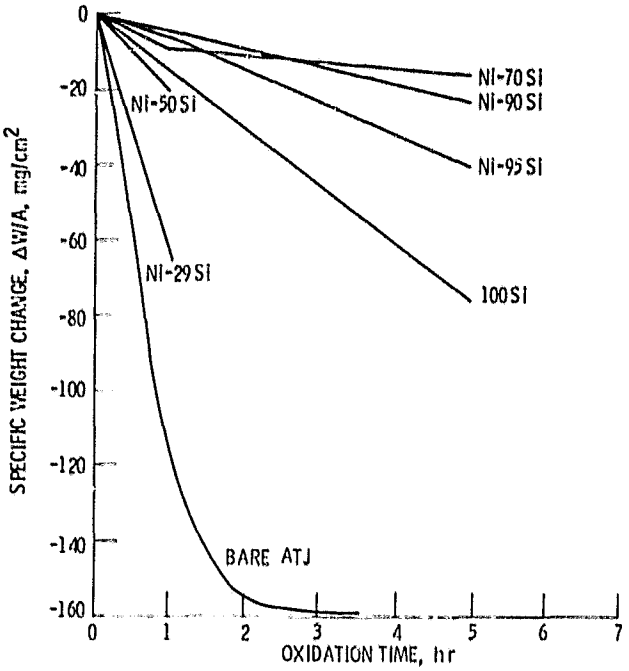

Figure 8. - Compositional effects on the 1200° C cyclic oxidation behavior of Ni-Si coatings (25 mg/cm^2).

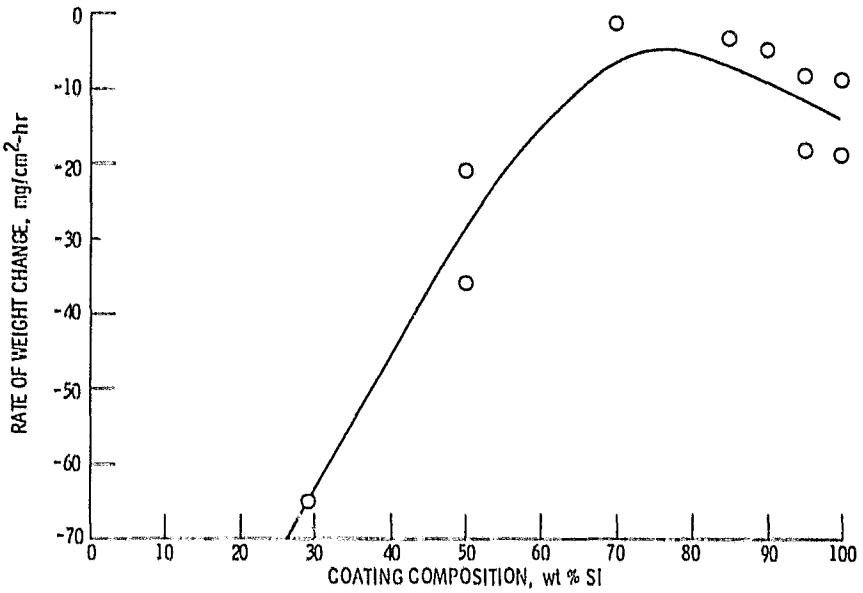

Figure 9. - Compositional dependence of oxidation behavior of Ni-Si coatings.

ORIGINAL PAGE IS
OF POOR QUALITY

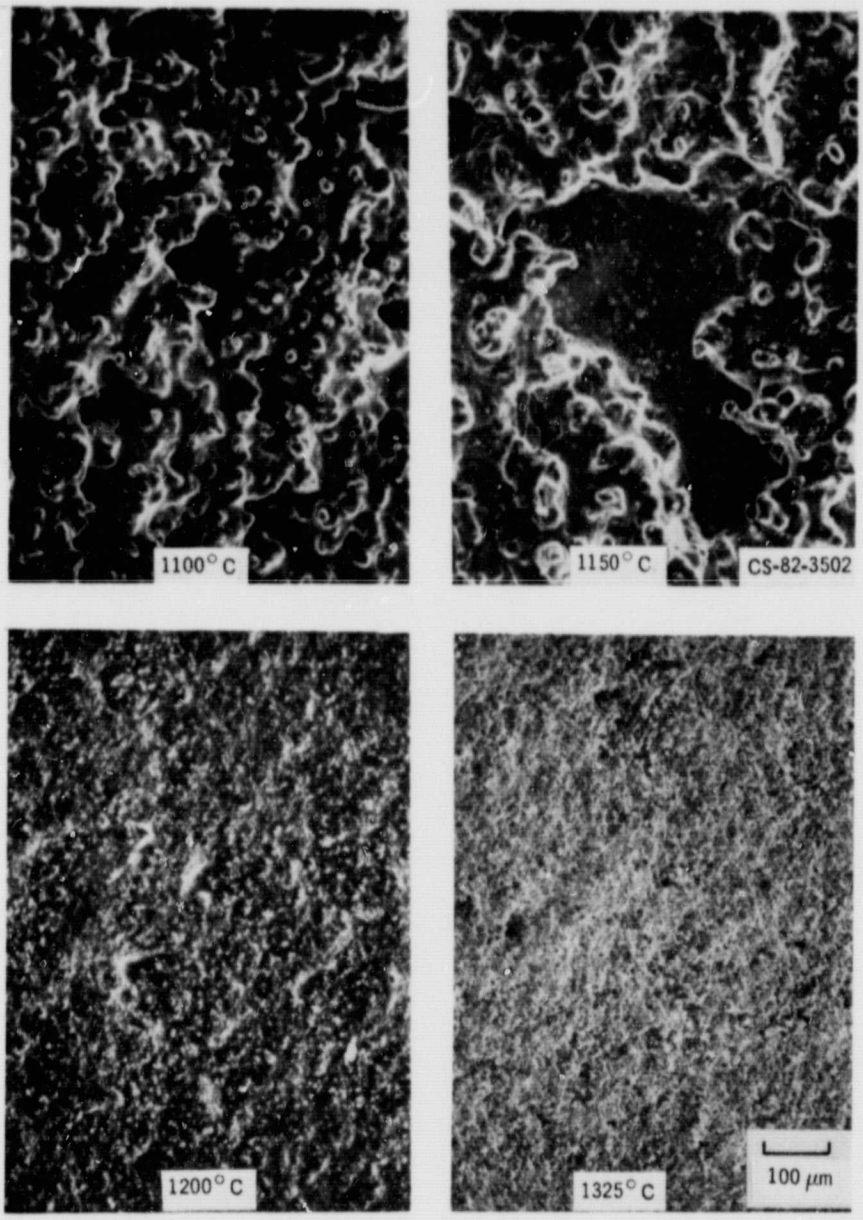

(a) Low magnification showing dramatic changes in surface roughness after sintering above 1200°C.

Figure 10. Ni-70 Si coating surface structure as a function of sintering temperature, 50 mg/cm^2, 1hr.

ORIGINAL PAGE IS
OF POOR QUALITY

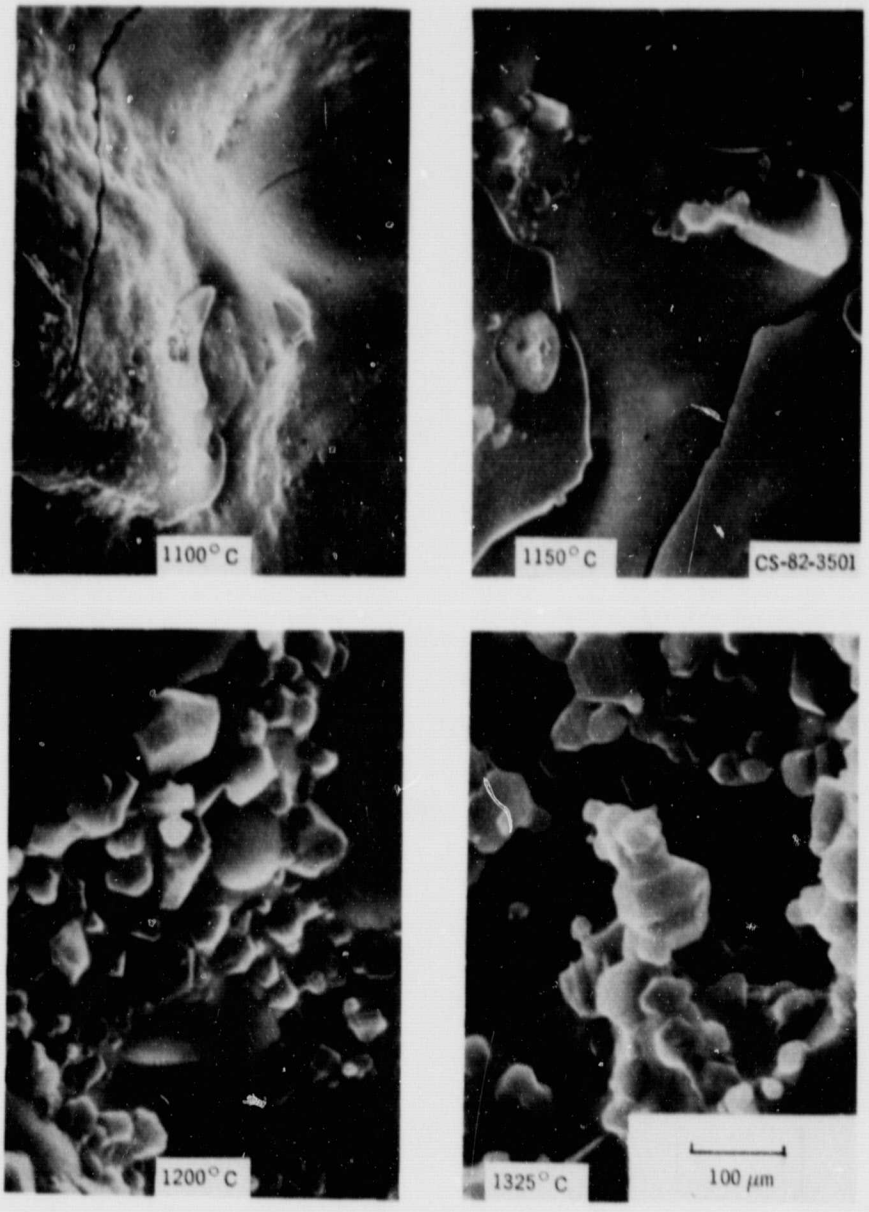

(b) High magnification showing increase in number of SiC crystallites.

Figure 10. - Concluded.

ORIGINAL PAGE IS
OF POOR QUALITY

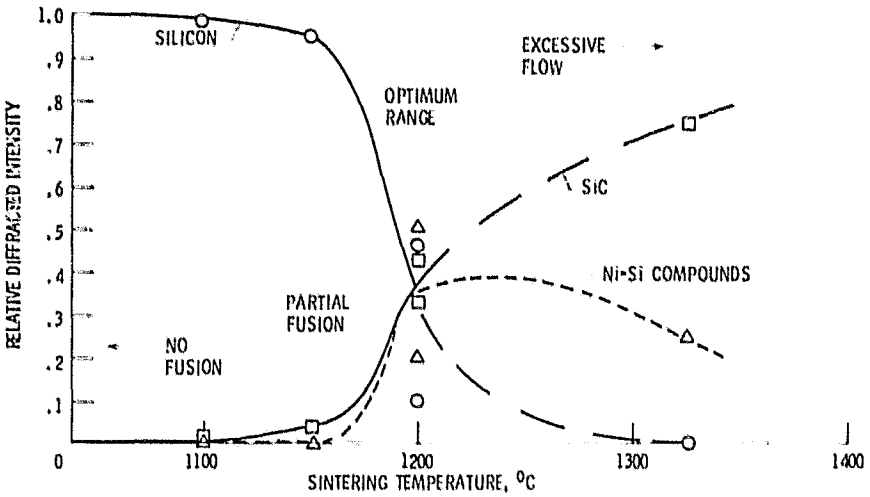

Figure 11. - Trends in estimated amounts of Ni-70 Si coating phases with sintering temperature (50 mg/cm^2, single-step for 1 hr.

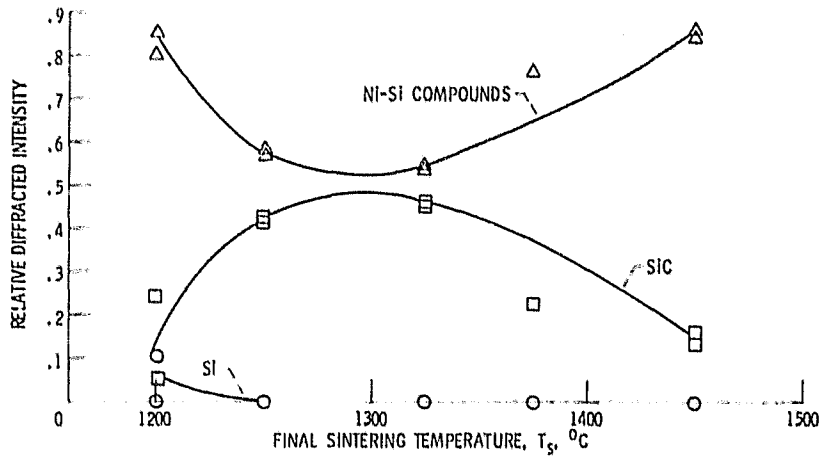

Figure 12. - Change in external coating phases with sintering temperature for the two-step Ni-70 coatings; 1200° C/1 hr + T_s/1 hr.

ORIGINAL PAGE IS
OF POOR QUALITY

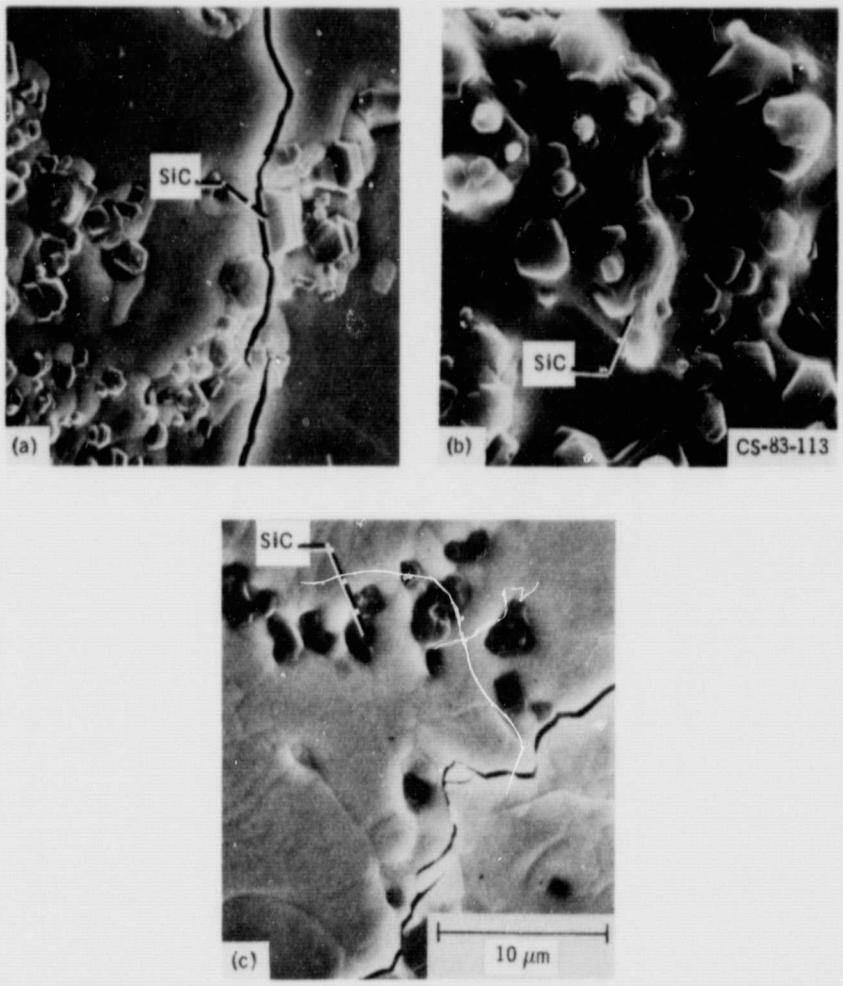

(a) 1200 C/1 hour + 1200 C/1 hour.

(b) 1200 C/1 hour + 1325 C/1 hour.

(c) 1200°C/1 hour + 1450°C/1 hour.

Figure 13. - Cracks and SiC crystallites in Ni-70 Si coatings sintered by the two-step process.

ORIGINAL PAGE IS
OF POOR QUALITY

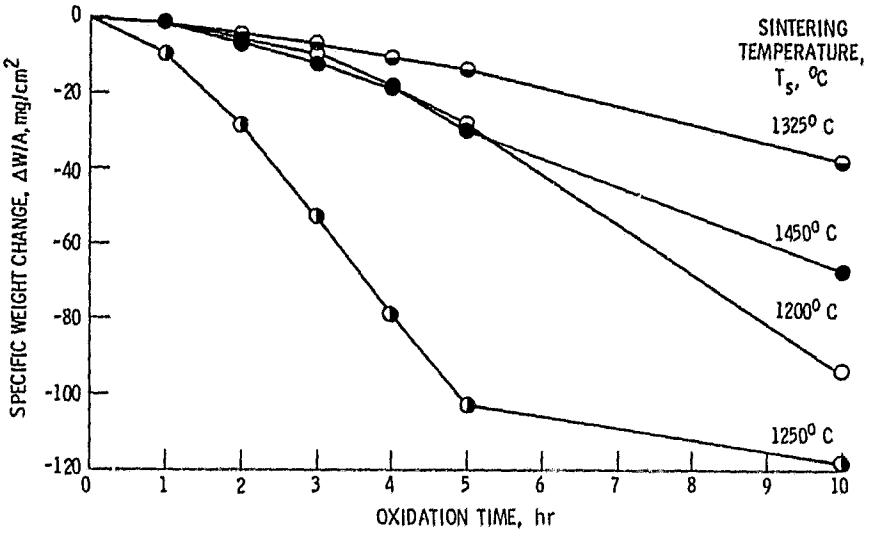

Figure 14. - 1200° C cyclic oxidation behavior of Ni-70 Si coatings sintered by the two-step process; 1200° C/1 hr + T_S/1 hr.

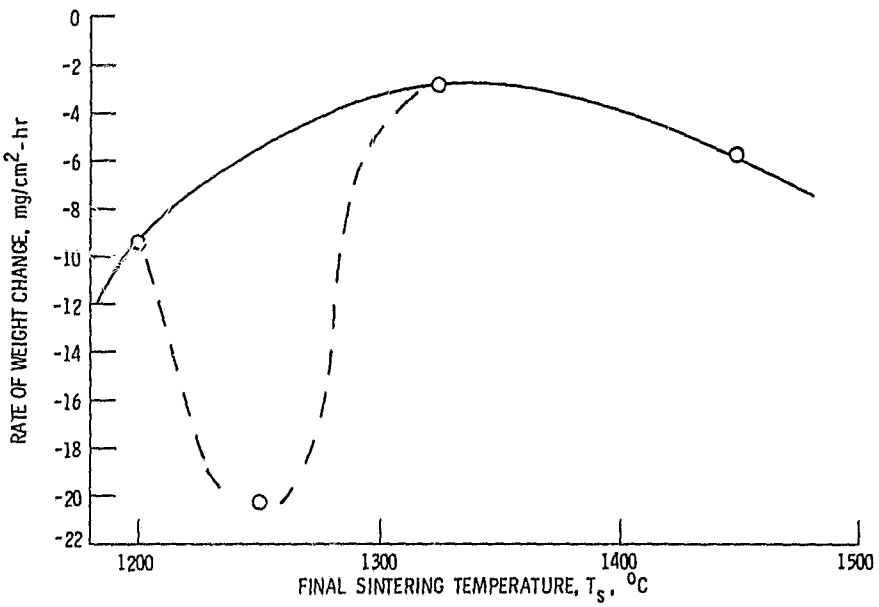

Figure 15. - Effect of sintering temperature on 1200° C oxidation behavior for Ni-70 Si two-step coating; 1200° C/1 hr + T_S/1 hr.

ORIGINAL PAGE IS
OF POOR QUALITY

(a) 1200°C/1 hour + 1200°C/1 hour.

(b) 1200°C/1 hour + 1325°C/1 hour.

(c) 1200°C/1 hour + 1450°C/1 hour.

Figure 16. - Surface microstructure of NiO crystallites (• SiO_2) formed on two-step Ni-70 Si coatings oxidized at 1200°C for 10 hour.

ORIGINAL PAGE IS
OF POOR QUALITY

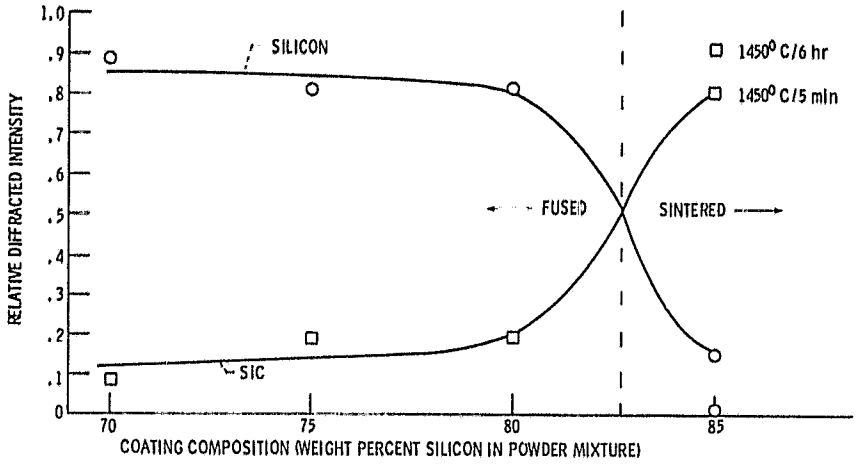

Figure 17. - Compositional effect on coating phases for short single-step process (1400° C/5 min.).

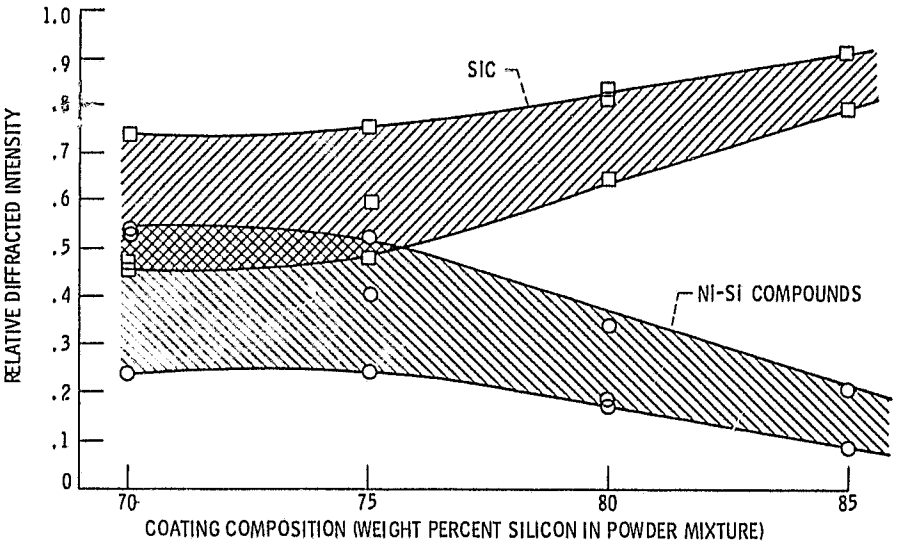

Figure 18. - Compositional effect on coating phases for long two-step process (1200° C/1 hr + 1325° C/1 hr.

ORIGINAL PAGE IS
OF POOR QUALITY

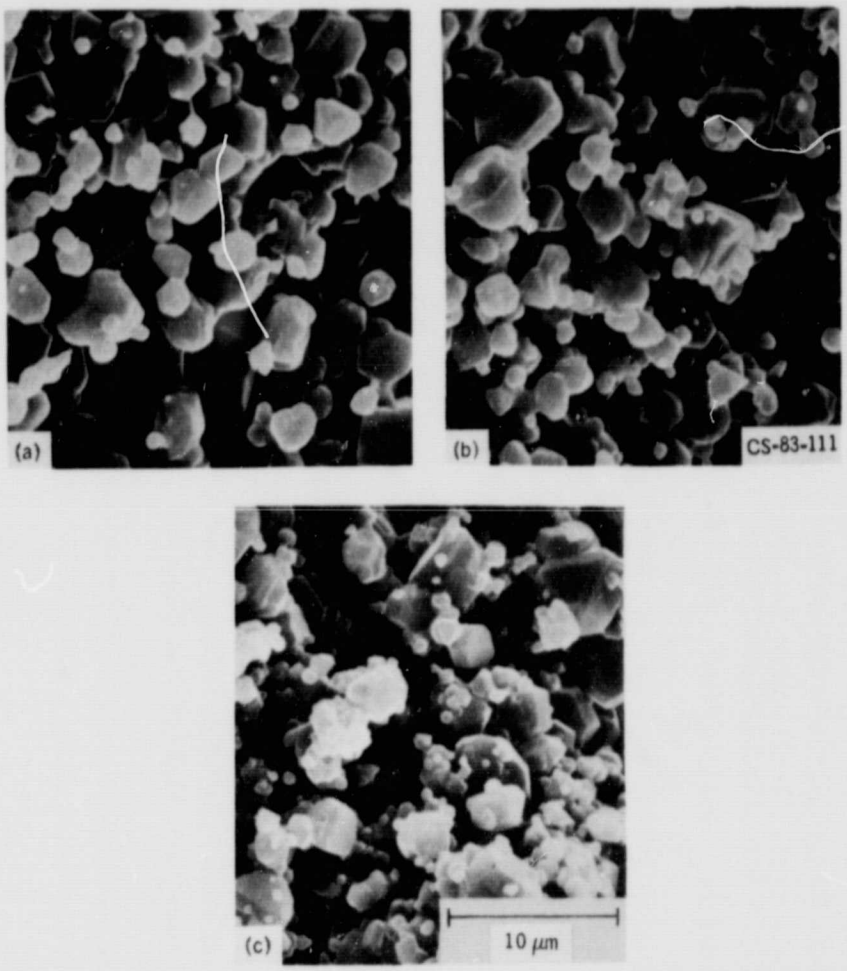

(a) Ni-75 Si.

(b) Ni-80 Si.

(c) Ni-85 Si.

Figure 19. - Effect of silicon content on surface microstructure of high-Si coatings sintered by the two-step process (1200 °C/1 hour + 1325°C/1 hour).

ORIGINAL PAGE IS
OF POOR QUALITY

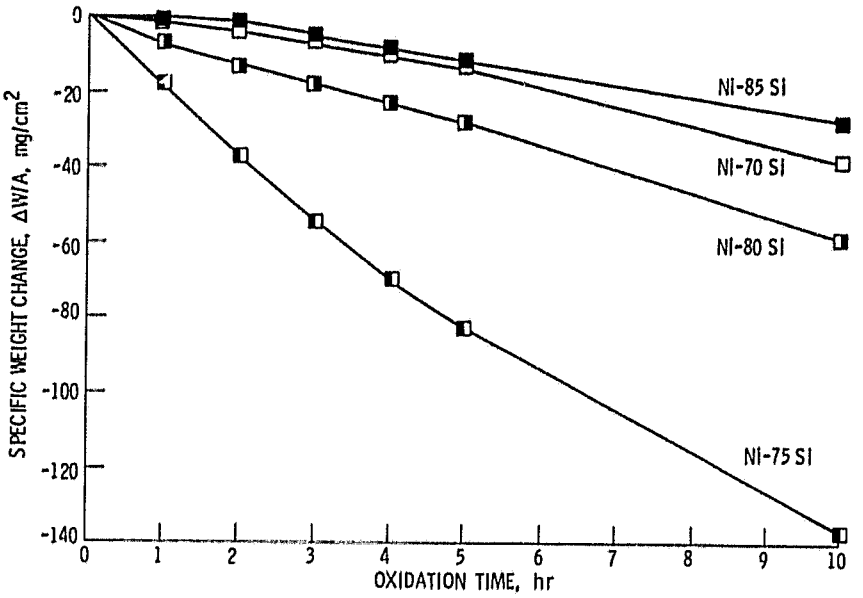

Figure 20. - 1200° C cyclic oxidation behavior of Ni-Si coatings sintered by the two-step process; 1200° C/1 hr + 1325° C/1 hr.

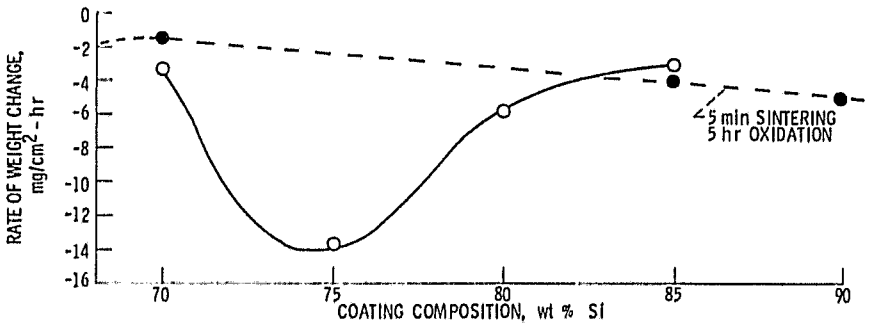

Figure 21. - Compositional effect on 1200° C oxidation behavior of the two-step Ni-Si coatings.

ORIGINAL PAGE IS
OF POOR QUALITY

(a) Ni-75 Si.

(b) Ni-80 Si.

(c) Ni-85 Si.

Figure 22. - NiO crystallites and SiO_2 surface oxides formed after 1200°C oxidation for 10 hours, high-Si coatings, two-step process.